

INSTRUMENTS AND METHODS OF INVESTIGATION PACS numbers: 07.07.Df, 07.57.Pt, **33.20.–t**, 87.85.Ox

Exhaled breath analysis: physical methods, instruments, and medical diagnostics

V L Vaks, E G Domracheva, E A Sobakinskaya, M B Chernyaeva

DOI: 10.3367/UFNe.0184.201407d.0739

Contents

Abstract. This paper reviews the analysis of exhaled breath, a rapidly growing field in noninvasive medical diagnostics that lies at the intersection of physics, chemistry, and medicine. Current data are presented on gas markers in human breath and their relation to human diseases. Various physical methods for breath analysis are described. It is shown how measurement precision and data volume requirements have stimulated technological developments and identified the problems that have to be solved to put this method into clinical practice.

1. Introduction. Exhaled breath analysis: general information

Exhaled breath (EB) analysis is a rapidly developing field of noninvasive medical diagnostics. As long ago as Hippocrates's time, doctors noticed that the exhaled breath of patients with diabetes mellitus, renal and hepatic disorders, or anaerobic infections is accompanied by a specific odor. This enabled them to diagnose the patient's state of health by smelling their EB. The key factor in the universal recognition of the value of this method was the work of Linus Pauling [1] published in 1971. It demonstrated that human EB is not merely a mixture of nitrogen, oxygen, carbon dioxide, and water. Pauling used gas chromatography to detect 250 more gases in EB.

To date, more than 800 gases have been identified among the products of physiological and biochemical processes in the human body. Their concentrations reflect the level of homeostasis, as well as the severity of pathological conditions [2]. Therefore, EB analysis can be used for diagnostic purposes, predicting a patient's response to a concrete therapeutic modality, and evaluating the effectiveness of the treatment.

Diagnostics based on EB analysis have a number of advantages over those using traditional laboratory methods. The analysis of gas mixtures is safe for medical personnel, since it does not require contact with biological fluids; moreover, it is relatively inexpensive, takes little time, and detects minimal amounts of the substances of interest. EB analysis is an ideal noninvasive monitoring (screening) tool and can be repeated arbitrarily many times for a detailed dynamic study of physiological processes. An extensive search for specific gas markers of various diseases is currently underway in clinics and universities in many countries (Netherlands, UK, Germany, USA, Israel). A large number of publications on EB analysis, the annual conference *Breath Analysis Summit*, and publications of the specialized *Journal of Breath Research* testify to extensive research activities in this field. They have yielded a vast database of the markers present in EB associated with various diseases. The best known ones are listed in the table (see [2] and the references therein). Moreover, commercial kits for the detection of selected EB gases have become

V L Vaks, E G Domracheva, E A Sobakinskaya, M B Chernyaeva
Institute for Physics of Microstructures, Russian Academy of Sciences,
ul. Ul'yanova 46, GSP-105, 603950 Nizhny Novgorod,
Russian Federation;
Lobachevsky State University of Nizhny Novgorod
(National Research University),
prosp. Gagarina 23, 603950 Nizhny Novgorod, Russian Federation
Tel. +7 (831) 417 94 57. Fax +7 (831) 417 94 64
E-mail: vax@ipmras.ru; elena@ipmras.ru

Received 8 May 2013, revised 11 October 2013
Uspekhi Fizicheskikh Nauk **184** (7) 739 – 758 (2014)
DOI: 10.3367/UFNr.0184.201407d.0739
Translated by Yu V Morozov; edited by A M Semikhatov

Table. Marker molecules in human EB and their diagnostic significance [2].

Molecule	Disease, stress factor, or physiological process
Hydrogen (H_2)	Digestive problems in babies Gastrointestinal disorders Carbohydrate malabsorption
Carbon monoxide (CO)	Anemias (hemolytic, sideroblastic, sickle-cell) Carboxyhemoglobinemia resulting from acute and chronic irradiation Long-term effect of enhanced O_2 level Neonatal hyperbilirubinemia Oxidative stress Hematomas, hemoglobinuria, preEB clampsia, infections, thalassemia Respiratory infection Asthma
Nitric oxide (NO)	Chronic obstructive pulmonary disease Asthma Hypertension Bronchectasis Upper respiratory tract infection Rhinitis Gastric inflammation (gastritis) including *Helicobacter pylori* infection Cancer of digestive organs Severe sepsis Chronic infectious inflammatory processes (gastritis, hepatitis, colitis)
Ammonia (NH_3)	Acute and chronic radiation disease Momoamine metabolism in the lungs Renal insufficiency associated with nephritis, hypertension, renal artery atherosclerosis, gestational toxicosis and nephropathy, toxic kidney lesions Hepatic insufficiency in various forms of non-toxic and toxic hepatitis and liver cirrhosis Lung cancer
Methane (CH_4)	Gastrointestinal disorders Carbohydrate malabsorption
Hydrogen peroxide (H_2O_2)	Compromised respiratory function Acute and chronic radiation disease Asthma
CS_2 and pentane	Schizophrenia
Ethylene (C_2H_4)	Oxidative stress, lipid peroxidation Inflammation (chronic asthma, inflammation of internal organs) Acute myocardial infarction Free radical-induced damage
Ethane (C_2H_6)	Vitamin E marker in children E-ubichinon status associated with lipid peroxidation Marker of free radical-induced damage
Ethane (C_2H_6) and pentane	Lipid peroxidation in liver transplantation Lipid peroxidation marker
Phenol (H_2CO)	Phenol pharmacokinetics and metabolism
Butane and pentane	Phenol pharmacokinetics and metabolism, liver diseases (cirrhosis, primary biliary cirrhosis, chronic active hepatitis, fatty degeneration)
Methanol Ethanol Acetaldehyde	CNS disorders Diabetes mellitus Alcoholism
Acetone	Pancreatic function in acute destructive pancreatitis and dietary imbalance Severe cardiac insufficiency Lung cancer
Pentane and its derivatives	Breast cancer Acute myocardial infarction Heart transplant rejection Rheumatoid arthritis Exacerbation of bronchial asthma
CO_2 isotopic modifications	Bacterial infection Hepatic dysfunction including cirrhosis Pancreatic dysfunction Lactose assimilation Malabsorption Bile metabolism Glucose metabolism

available, together with clinically tested methods for the diagnostics of a number of disorders based on EB analysis.

2. Recent achievements in and problems concerning exhaled breath analysis: clinical aspects

2.1 Diagnostics and monitoring of respiratory diseases

Respiratory diseases (RDs) are the most common pathologies. In Europe, they are ranked second after cardiovascular disorders among the leading causes of death [3]. The incidence of inflammatory conditions, such as asthma and obstructive pulmonary diseases (OPDs), has increased significantly in recent decades despite the decreased frequency of lung infections including tuberculosis and pneumonia [4]. Chronic respiratory disorders are currently a major challenge to modern medicine. In the USA, OPDs are fourth on the list of diseases with a lethal outcome. In Italy, 2.6 m people suffer from OPDs that cause 18,000 deaths per year. Bronchial asthma affects people of any age; its prevalence increases in children, and mortality from this pathology has increased by 42% during the last 10 years [5]. The causes of asthma vary, which hampers elucidation of the mechanisms underlying this condition.

A variety of methods have been proposed for the diagnostics and monitoring of asthma and OPDs [6]. Testing lung function reveals pathological changes in static and dynamic lung volume and pulmonary gas exchange. Radiological technologies, in the first place high-resolution computed tomography, provide information on lung tissue degeneration. However, these methods allow only indirect evaluation of the long-term injurious action of toxins and poisons.

It is widely believed that inflammation is responsible for bronchial hypersensitivity, obstruction of incoming air flow, and mucus hypersecretion. This opinion motivated extensive studies aimed at identifying the inflammatory cells and mediators involved in the cascade of processes linking the triggering stimulus with the final abnormal state of the airways.

It has been shown that such conditions have a variety of manifestations at the cellular, anatomical, functional, and clinical levels, which allows distinguishing different phenotypes. Moreover, the severity of a disorder depends not only on the lung function evaluated by spirometry but also on clinical symptoms, complications, and concomitant pathologies, which provides a basis for differentiation among the phenotypes. The differences among phenotypes, in turn, create prerequisites for the choice of a therapeutic strategy and prediction of the patient's response.

A large number of biomarkers have been identified in human EB, saliva, and blood that help to elucidate mechanisms of asthma and OPD, choose an adequate treatment, and predict its outcome. Nitric oxide (NO) has been shown to be the most valuable of them in terms of the amount of information it contains.

The first work on NO detection in EB dates back to the 1990s. Hemiluminescence techniques were employed to show that the EB of asthmatic patients exhibits an enhanced NO level that decreases under the effect of corticosteroid therapy [7, 8]. This work gave evidence that measurements of NO content in EB can be used as a diagnostic tool for asthma and to monitor response to anti-inflammatory therapy. Such measurements yield information about inflammatory processes in the airways that cannot be obtained by traditional methods, e.g., spirometry, characterizing only their reactivity.

However, a number of problems have to be resolved before NO analysis is introduced in routine clinical practice [9]. These are (1) better understanding the role of NO in pathological processes leading to the development of asthma; (2) standardizing methods and instruments for the measurement of NO levels; (3) organizing a large-scale examination of asthmatics for the identification of interfering factors and determining the clinically significant range of NO concentrations; (4) elaborating a strategy for the interpretation of the results obtained. Some of these issues have been successfully addressed, while resolving others is underway.

The key factor in advancing NO analysis in clinical settings was the standardization of NO measuring methods in the EB of adults and children undertaken in Europe and the USA in 1997 and 2005 [10, 11]. It opened up prospects for the extensive collection of data on the NO concentration in the EB of asthmatic patients. As a result, guidelines for using NO measurements in clinics and hospitals were developed. They are currently being updated. Diagnostics and monitoring of asthma based on the NO level in EB are widely used in American medical facilities.

OPD monitoring is likewise based on the NO levels in EB from the peripheral respiratory tract (bronchioles) as the major site of inflammation and obstruction. Methods for differential measurements of EB components from alveoles and large lung compartments at different EB flow rates were recently described in Ref. [12]. They permit measuring four parameters: the alveolar or peripheral NO level, the airway diffusion capacity, the stationary NO concentration in different airway segments, and the maximum NO flow across airway walls. It is demonstrated in [13] that a correlation exists between peripheral NO levels and the functional status as well as between NO levels in large lung compartments and the general health status of patients exhibiting stage 3 and 4 OPD.

Studies on noninvasive diagnostics of OPD and asthma are underway based on the analysis of EB condensate prepared by EB freezing [14]. Such an analysis is already performed in clinical settings to measure airway acidity and evaluate indicators of inflammation (adenosine, ammonia, hydrogen peroxide) [15]. Concentrations of these substances are shown to depend on the type of pathology (asthma or OPD) and its severity.

Another dangerous disease of the respiratory system is lung cancer. The risk group largely comprises smokers, whose number has increased throughout the world. In nonsmokers, lung cancer is the fourth leading cause of death following prostate, colon, and breast cancer [16]. Lung cancer is curable if it is caught at an early stage. However, such cases are rare (not more than 20–30%), and only 5% of patients live for about 5 years after their cancer is diagnosed. The US program for lung cancer screening with computed tomography (CT) and radiography helped detect the disease in high-risk groups [17]. The program involved 53,000 subjects who were regularly examined for two years. The early detection of lung cancer allowed the mortality rate to be reduced by 20%.

However, low-dose X-ray screening has disadvantages. First, most of the small nodules visible on an image are benign, which requires an additional diagnostic procedure, a biopsy study, to be performed to confirm the diagnosis. Second, irradiation itself increases mortality by 0.01% to several percent. Finally, 75% of patients develop lung neoplasms (nodules) [18, 19]. Although these tumors prove benign, their role in further malignization remains to be clarified.

Importantly, such diagnostics are expensive. Therefore, a readily available and rapid screening technique that is safe for the patients and the medical personnel is needed for the early detection of lung cancer. The first work on spectroscopic analysis of EB composition in patients with this pathology have already been published (see, e.g., [20–24]). Specifically, it was shown by mass spectroscopy [20] that the EB of lung cancer patients contains a stable set of volatile organic substances, mostly alkane derivatives. These markers were used to develop a diagnostic test for lung cancer with a sensitivity of 84.6% and specificity of 80%. The results of the analysis were unrelated to the cancer stage and smoking behavior.

A recent paper [25] describes a preliminary model for the detection of lung cancer based on the identification of 22 volatile organic substances (13 aliphatic and aromatic hydrocarbons, 9 linear aldehydes) and hydrogen peroxide in EB condensate. Sensitivity of the analysis was estimated at 83.9% and specificity at 71%. Nevertheless, further studies are needed, despite the large number of publications, because different authors use different sets of marker gases for cancer diagnostics; meanwhile, the clinical application of this diagnostic method implies the use of a universal and reproducible set of markers.

EB of patients with malignant pleural mesothelioma (MPM) is worthy of special mention. The etiology of this aggressive tumor is related to the long-term impact of asbestos fibers. Therefore, the authors of [26] used chromato-mass-spectrometry to study EB composition in three groups of subjects: (1) patients with MPM, (2) subjects exposed to the impact of asbestos, either at present or in the past, and (3) healthy people unaffected by asbestos dust. It was shown that MPM patients, unlike subjects of other groups, had cyclopentane in their EB. Moreover, the presence of cyclopentane may indicate a long-term effect of asbestos dust, since it was found only in group 2.

2.2 Diagnostics of other diseases

Another field where EB analysis is extensively employed is the diagnostics of helicobacteriosis.

An important achievement of modern physiology and medicine is the discovery of the pathogenic role of *Helicobacter pylori* in gastroenterology. Experts from the World Health Organization (WHO) maintain that almost 80% of patients with chronic gastritis and peptic ulcers are infected with H. pylori; hence, the importance of the diagnostics of this infection. The major tool for this purpose is the urea breath test (UBT), in which an enzyme called urease specifically breaks an aqueous carbamide solution down into ammonia and carbon dioxide [27–29]. To facilitate the identification of the resultant carbon dioxide, carbamide with a modified isotopic composition is administered into the stomach at a dose of 1 mg/kg body weight and ^{13}C-labeled carbon dioxide is determined in the EB by mass spectrometry.

Despite a number of advantages over traditional invasive bacterial tests, UBT has an important drawback: its sensitivity is limited by natural variations of the carbon-13 content in EB during analysis. This hampers only early diagnostics of H. pylori infection and the monitoring of its treatment. Moreover, 13-carbon UBT requires expensive equipment and reactants. It can be modified by using ammonia as the marker, the amount of which in the human body is a few orders of magnitude smaller than the natural background level of carbon-13. The practicability of such an approach was demonstrated in [30]. Noninvasive diagnostic methods are currently in demand for the study of other gastrointestinal diseases.

Crohn's disease and ulcerative colitis are chronic gastrointestinal disorders referred to as inflammatory bowel diseases (IBDs). The possibility of differential diagnoses between these conditions arises from the differences among their clinical pictures and, therefore, different therapeutic strategies. In most cases, the diagnosis is based on endoscopic examination of intestinal mucosa and the treatment end-point is its healing. However, ileocolonoscopy is a time-consuming invasive method apt to produce undesirable side effects. Moreover, it sometimes fails to reveal microscopic inflammation sites in the bowel.

Thus far, several articles on IBD diagnostics with the help of EB analysis have been published [2, 31, 32]. The authors of [2] describe tissue lesions associated with ulcerative colitis that can be detected based on the analysis of lipid peroxidation products in EB, which confirms the hypothesis of the role of lipid peroxidation in IBD pathogenesis. The EB ethane level was found to positively correlate with the results of endoscopic examination and clinical manifestations of the disease. The detection of IBD markers by gas chromatography in 20 patients, including 10 with Crohn's disease and 10 with ulcerative colitis, is reported in [31]. The EB of IBD patients contained ethane, propane, and pentane in higher concentrations than in healthy subjects. The results of these studies indicate that excessive lipid peroxidation is an important pathogenetic factor of IBD that can be identified by the noninvasive diagnostic method under consideration. At the same time, the above markers proved to be insufficiently sensitive and specific for differentiating among various forms of IBD. The analysis of volatile organic substances in the EB of patients with IBD was extended in [32] using gas chromatography in combination with time-of-flight mass spectrometry. The study demonstrated that EB analysis can be used to differentiate between active and inactive forms of the disease. Further studies aimed at developing EB analysis for the differential diagnostics of IBD are currently underway.

Another example of EB analysis for the diagnostics of intestinal pathology is the detection of malabsortion, a state arising from abnormalities in absorption and transport across the mucous membrane of adequately digested food nutrients (carbohydrates, proteins, fats, vitamins, and microelements) [33]. One of the tests for carbohydrate (lactose, fructose, sorbitol) malabsorption in the small intestine is a hydrogen breath test, which reveals that carbohydrates fail to pass from the small intestine into the colon; since carbohydrates make a substrate for colonic bacteria, the result is excessive bacterial growth. Carbohydrate fermentation products include short-chain fatty acids (SFAs), carbon dioxide, methane, and hydrogen. The last of these traverses the intestinal wall, enters the systemic circulation, and is then carried through blood vessels to the lungs. We recall that hydrogen is not released by cells and appears only as a product of the anaerobic bacterial metabolism of carbohydrates, meaning that practically all hydrogen exhaled by a person results from anaerobic activity of colonic bacteria. Procedures for hydrogen breath tests are fairly well developed and universally applied.

The possibility of using EB analysis for intestinal cancer diagnostics was evaluated in [35] with the use of chromatomass-spectrometry. The authors identified 15 substances (nonanal, 4-methyl-2-pentanon, decanal, 2-methylbutane, 1,2-pentadien, etc.) whose presence distinguishes the affected patients from healthy subjects with a probability of 76%.

Modern methods for the treatment of diabetes mellitus and its complications are based on the regular control of blood glucose, insulin, and lipid levels. Such monitoring is inconvenient for the patients, includes painful injections, and leads to callus formation at sites of frequent blood sampling. EB analysis for the presence of volatile organic substances may be an alternative to this approach. It has long been known that the EB of diabetic patients contains ketones, and these compounds have been studied for many decades with a view to using them for diagnostics of diabetes. The work was hampered by the absence of highly sensitive methods for gas analysis. Recent progress in analytical techniques has provided a basis for designing instruments with a sensitivity of 10 ppt (parts per trillion, 10^{-12}). A method was proposed for indirect estimation of blood glucose, insulin, and lipid levels from the presence in EB of two sets of organic substances: one comprises acetone, methylnitrate, etanol, and ethylbenzene, and the other 2-penthylnitrate, propane, methanol, and acetate. It was shown that concentrations of these compounds in EB are in excellent agreement with the results of biochemical analysis. Optimization of calibration procedures and prognostic algorithms, as well as the development of cheap sensors, may significantly promote the wide application of this method in clinical practice.

To conclude this section, it seems appropriate to quote the results of an interesting study devoted to diagnostics of nervous system diseases. The authors of [37] considered the possibility of diagnosing Parkinson's disease (PD) and Alzheimer disease (AD) by detecting marker gases in EB. The study involved 57 subjects, including patients with PD and AD, besides healthy persons. It demonstrated the possibility of differentiating among the three groups and also between early and late stages of PD.

3. Physicochemical methods of gas analysis and major requirements for the instruments for exhaled breath analysis

3.1 Analytical methods for studying many-component gas mixtures

All known methods can be divided in terms of the origin of an analytical signal into chemical, physicochemical, and physical [38].

Chemical methods utilize donor–acceptor reactions with proton (acid-base), electron (redox), and electron pair (complex formation) transfer, as well as precipitation–dissolution and extraction processes.

Physicochemical methods are divided into electrochemical, spectroscopic (optical), luminescent, kinetic, and thermometric. They measure an analytical signal generated with the participation of outer (valence) electrons and functionally related to the nature and concentration of the substance. The signal arises from the interaction of matter with various forms of energy (electrical, thermal, electromagnetic, etc.). To produce a signal, the study component is frequently converted from one form into another, more convenient for the method in use. For example, in photometric and luminescence analysis, the substance of interest is transformed into one with higher absorptivity or a higher quantum yield.

Physical methods include spectroscopic (nonoptical), nucleophysical, and radiochemical methods recording an analytical signal produced with the participation of inner electrons or atomic nuclei.

The main characteristics of the analytical methods are listed below.

1. *Sensitivity* (or detection limit) — the lowest concentration of an analyte that can be determined to be statistically different from a blank. Usually, the concentration of gases is measured in ppm (parts per million, 10^{-6}), ppb (parts per billion, 10^{-9}), or ppt.

2. *Selectivity* — the ability to determine the presence of molecules (or atoms) of a given type in their mixture. This characteristic first of all directly depends on the ability to distinguish between nearby peaks (absorption lines or bands) suggesting the presence of various substances. Moreover, it is necessary to ensure unambiguous and reliable identification of all registered peaks (absorption lines or bands).

3. *Reproducibility* — the parameter reflecting random measurement errors and showing the scatter between repeated measurements.

4. *Temporal resolution* — the minimal time interval detectable in a useful signal. This interval depends on the performance characteristics of the spectrometer detection system and is directly related to its operational speed. Temporal resolution is crucial for the detection of short-lived compounds and the development of online methods for the analysis of gas mixtures.

5. *Spectral resolution* (*for spectroscopic methods*) — the minimal frequency interval in the substance spectrum detectable by the apparatus. Spectral resolution directly determines the possibility of differentiation between absorption lines at similar frequencies; in other words, it is related to the selectivity of the analysis. In classical gas spectroscopy, spectral resolution is limited by the instrumental resolution of the spectrometer.

EB is a complex analytical object containing different amounts of organic and inorganic substances. It requires the application of up-to-date methods of gas analysis satisfying rigorous analytical criteria. The most effective physicochemical methods for EB analysis include

— chromatographic methods utilizing sorption processes;

— electrochemical methods based on the electrochemical properties of analyte gases.

Physical methods for EB analysis are infrared (IR) and terahertz spectroscopy based on the interaction between matter and electromagnetic radiation.

3.2 Major requirements for instruments and methods for exhaled breath analysis in clinical settings

Despite a number of advantages inherent in EB analysis, its extensive application in clinical settings is hampered by the following factors:

• the lack of adequate information about a stable set of markers of many diseases or pathological conditions and their direct relationship with physiological processes;

• the absence of suitable instrumental methods of EB analysis for laboratory studies and clinical applications.

Therefore, physicists, engineers, and the health care professionals are faced with three main groups of problems:

1. The search for and biochemical substantiation of a stable set of marker molecules for a concrete disease.

2. The development of analytical methods for the detection of marker molecules using detailed information on the spectra and detection limits.

3. The creation of adequate methods for the identification of marker molecules based on the available technologies and detection limits.

We consider the main requirements for the characteristics of the instrumental method for EB analysis. The difficulty of development of such instruments arises from the necessity to combine the following important parameters in a single device.

1. *Possibility of simultaneous measurement and identification of several molecules*. As is known, the high degree of confidence of a diagnosis is ensured by registration of the entire set of marker gases, because no single biomarker is 100% specific [39].

2. *High sensitivity and accuracy of concentration measurements*. Most markers are present in EB at a concentration of 10 ppt–10 ppm. The measurement accuracy is 3–5% because of variations in breathing and blood flow rates.

3. *Selectivity*. Inasmuch as EB contains tens of gas species, its analysis must ensure the reliable detection and identification of the substances of interest, despite high concentrations of nitrogen, oxygen, water, and carbon dioxide. Poor selectivity decreases the degree of confidence and the accuracy of diagnosis.

4. *Operational speed*. In most cases, an operational speed up to hundredths of a second in online measurements is needed [41]. The overall time of analysis with averaging over several exhalations is around 5–10 s.

5. *Easy handling*. The instrument is easy to use and has a simple, clear interface, which is of primary importance in clinical applications.

6. *Cost of a single measurement and of the instrument*. Extensive application of EB analysis implies the availability of inexpensive equipment and reactants.

4. Commercial exhaled breath analyzers

This section presents examples of commercial gas analyzers designed for recording biomarkers in EB. Such devices are equipped with special tubes and bags for EB sampling, systems for the incoming airflow control, and data processing systems. Standard breath alcohol meters for ethanol measurement are not considered here.

The following analytical regimes are feasible, depending on the type of instrument:

• *online measurements* using an inbuilt system for feedback airflow control, including a flowmeter (a constant airflow velocity in the range 10–100 ml s^{-1});

• *off-line measurements* with air sample collection in special bags for subsequent analysis;

• analysis of EB from the nasal cavity based on a special breathing technique to ensure a constant airflow through the nasal cavity at a speed of 3 l min^{-1};

• '*inhalation-exhalation*' *measurements*. This method is designed to analyze EB in those cases where online measurements are impracticable (young children, animals). Instruments for the purpose are equipped with a pressure sensor and a control system that determines the end and the beginning of each exhalation and calculates the concentration of biomarkers.

Modern commercial exhaled breath analyzers are available as gas analyzers utilizing electrochemical sensors and chemiluminometers.

Gas analyzers using electrochemical sensors (ECSs) with a sensitivity of 1–5 ppm, an accuracy of 2–5% , and a response time of a few dozen seconds (Bedfont Scientific, Ltd., UK) detect H_2, CO, and NO [42–45]. These analyzers record an electrical signal between the electrodes when the gas enters the sensor. The main ECS elements are a working electrode and a counter electrode separated by an electrolyte layer [46] (Fig. 1).

The auxiliary elements include capillaries and a hydrophobic membrane to control the amount of gas reaching the working electrode and to prevent electrolyte leakage. The gas enters the ECSs as it diffuses through small capillaries toward the hydrophobic membrane and then to the working electrode, where it undergoes a redox reaction along the reductive or oxidative pathway. The reaction is catalyzed by an electrode material specially selected for the gas of interest. The chemical reaction generates an electric current proportional to the gas concentration, flowing through a resistor placed between the cathode and the anode. Many sensors in which an external command voltage is used have an additional (reference) electrode to maintain a constant potential on the working electrode varying under the effect of chemical reactions. The reference electrode to which a fixed potential is applied is placed near the working one such that there is no current between these electrodes.

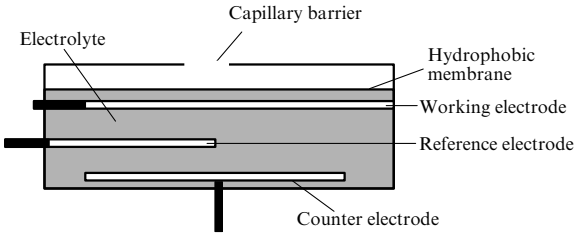

Figure 1. Typical electrochemical sensor.

As an example, we consider O_2 sensors that are currently believed to be the best type of ECS due to the high sensitivity, selectivity, and confidence. Such ECSs have two Pb- (or Cd-) electrodes. In the course of an oxidation reaction, electrons emitted from the anode reach the cathode through the external circuit to induce the reduction of oxygen.

Oxidation on the anode in an acidic electrolyte:

$$2Pb + 2H_2O \rightarrow 2PbO + 4H^+ + 4e^- ,$$

reduction on the cathode:

$$O_2 + 4H^+ + 4e^- \rightarrow 2H_2O .$$

Oxidation on the anode in an alkaline electrolyte:

$$2Pb + 4OH^- \rightarrow 2PbO + 2H_2O + 4e^- ,$$

reduction on the cathode:

$$O_2 + 2H_2O + 4e^- \rightarrow 4OH^- .$$

Overall chemical reaction:

$$2Pb + O_2 \rightarrow 2PbO .$$

The advantages of ECS-based analyzers include compactness, easy handling, and low energy consumption. Their selectivity depends on the sensor type and the nature of the gas. Oxygen sensors are ranked among the best ECSs, because others produce noise signals of interfering gases. For CO, such gases are H_2S, SO_2, NO, NO_2, and H_2. The special choice of the electrode material allows selectively detecting a given gas.

'The gold standard' for nitric oxide (NO) detection is the chemiluminescence technique. Many instruments for the method are currently on the market, e.g., by Medics ECS (Switzerland) and General Electric (USA). Their sensitivity is < 1 ppb and and response time around 1 s. A typical chemiluminometer (CL) placed in a lightproof container consists of a sample chamber, reaction cell, sampling inlet, mixer, detector, and data collection and processing system (Fig. 2).

The container serves to maintain the desired temperature and protect the detector from light. The sample chamber contains a cell for the chemical reaction between the analyte and a special reactant. Emission released in the reaction is recorded by the detector. The concentration of the analyte gas is determined from the signal intensity.

The following reaction is used to detect NO [52]:

$$NO + O_3 \rightarrow NO_2 + O_2 .$$

The NO_2 gas formed in this reaction emits in a wide range and passes from the excited state to the ground state. Radiation in the UV range is registered by a photon counter.

Chemiluminometers are official devices for online measurements of NO in EB [53]. Due to this, they are often used to analyze and verify the performance efficiency of other instruments. For example, a commercial ECS and a standard chemiluminometer are compared in Ref. [54].

The principal disadvantage of CLs is the use of a destructive analytical procedure. For this reason, the realiza-

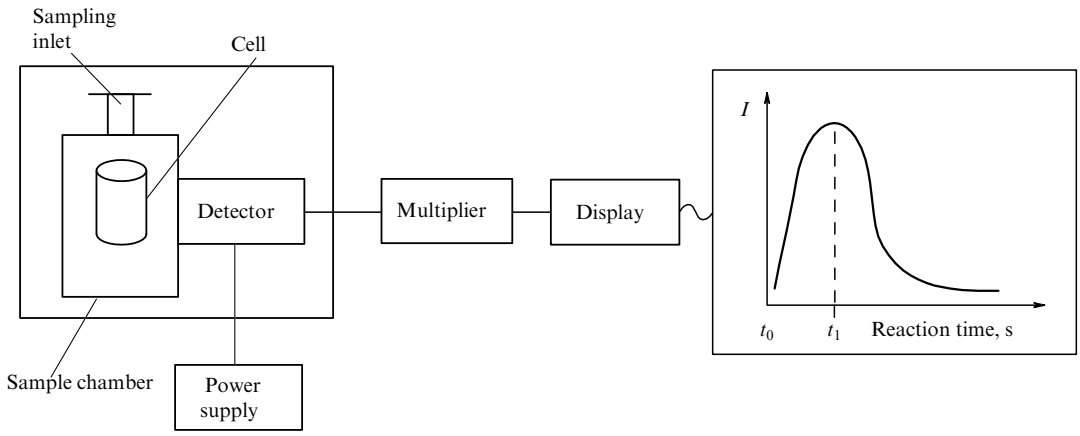

Figure 2. Block diagram of a chemiluminometer.

tion of several controllable reactions and the reliable interpretation of their results for a set of biomarkers in a many-component gas mixture seem an unlikely possibility. Moreover, the combustion of a many-component gas mixture in ozone may result in uncontrollable distortion of its composition, including the composition percentage of the analyte gas. Another drawback of CL-based instruments is the necessity of frequent calibration and maintenance operations that increase the cost of analyses.

The above gas analyzers are characterized by high sensitivity, rapid response, and a sufficient accuracy and selectivity of analysis. We recall that CL- and ECS-based methods cannot be used for simultaneous registration of several substances. Gas analyzers for the detection of several biomarkers must include a sensor array system [55]. But even then, the number of analytes to be detected is limited, because ECS methods are designed for the detection of simple inorganic compounds, such as O_2, H_2, CO, NO_x, HCs, SO_x, CO_2, NH_3, and H_2S [56]. Similar limitations hold for CLs used to detect NO, NH_3, SO_2, and O_3.

The advent of infrared semiconductor lasers gave a powerful impetus to the development of IR spectroscopic techniques for EB analysis. They are used in breath alcohol meters to measure ethanol in EB. Another example of the application of IR spectroscopy is a series of carbon dioxide $C^{13}O_2$ detectors (Wagner Analysen Technik, Germany), allowing measurements in the gas concentration range from 0.5 to 5.0 volume percent. Analysis of a single sample takes 2 minutes. Similarly to CL- and ECS-based gas analyzers, IR spectroscopic detectors are optimized for single-gas detection, which considerably restricts their application.

An analysis of commercial options shows that the major challenge to EB analysis is currently the development of instruments capable of detecting a set of marker gases. Methods of gas analysis most suitable for the detection of EB constituents are discussed in Section 5.

5. Modern gas analyzers

Only a few modern physicochemical methods for the detection of trace quantities of gases are suitable for EB analysis. They include gas chromatography (GC), mass spectrometry (MS), gas chromatography/mass-spectrometry (GC/MS), and IR spectroscopy (IRS). Appreciable progress in spectroscopic analysis is expected from the development of terahertz spectrometers.

5.1 Gas chromatography

In gas chromatography (GC), a sample and a carrier gas (hydrogen, helium, nitrogen, argon, carbon dioxide) are passed together through a chromatographic column [57]. Each substance takes a different amount of time to pass through the column, which results in their separation into fractions. Highly soluble components need more time than poorly soluble ones to be eluted from the liquid phase. The output detector registers foreign gases in the carrier gas. Each substance is identified from its elution time, and its amount as determines from the peak duration and intensity. Gas chromatography is used for the qualitative and quantitative determination of individual components in mixtures of organic and inorganic gases, liquids, and solids. Plasma-ionization, plasma-photometric, and photo-ionization detectors, as well as electron capture detectors are used. A GC analysis has a sensitivity of $1–10^3$ ppb, but the selectivity of many methods is poor. The accuracy is 10^{-6} %. The limiting factors are the low volatility and stability of analytes. Essential disadvantages of GC are the complicated sample preparation technique (preliminary concentration of the sample and/or reduction of its size) and the long (a few minutes) separation cycle, which does not permit using this technique for online measurements and monitoring. These drawbacks restrict its application in laboratory research.

In EB analysis, GC is largely used to detect volatile hydrocarbons, such as ethylene (C_2H_4), ethane (C_2H_6), propane (C_3H_8), pentane (C_5H_{12}) [31, 58], acetone [59], and hydrogen sulfide [60].

5.2 Mass spectrometry

Mass spectrometry (MS) [61] determines the ion mass-to-charge ratio m/q, which requires preliminary ionization of the substance to be detected. A variety of ionization processes are known: electron impact, chemical, field, and laser ionization. The ions thus created are separated and identified. Separation is based on the difference between ion paths in a magnetic and/or electrostatic field. The ions are identified with the use of photomultipliers. Advantages of such spectrometers include versatility, rapid response, and high sensitivity, amounting to a few ppb. The accuracy ranges from several percent to tenths of a percent. Moreover, it is difficult to identify individual gases in complex mixtures, because a given mass-to-charge ratio may correspond to more than one ion species or molecular fragments. Mass spectrometry is usually

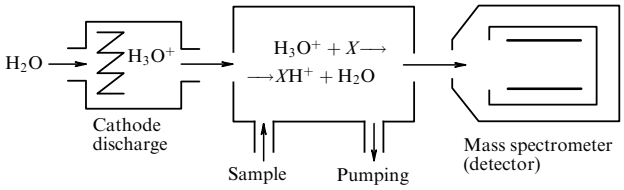

Figure 3. Block diagram of PTRMS. X is the analyte.

combined with other methods to improve the selectivity of analysis.

The possibility of combining MS and the soft ionization method based on the proton transfer reaction (PTRMS) for the detection of acetone and isoprene in EB was demonstrated in [62–64]. A special reactant for soft ionization (usually H_3O^+) interacted via proton transfer with all substances showing an affinity for protons higher than that of water (Fig. 3).

The ionized molecules were accelerated by an electric and/or magnetic field and detected by MS. The advantages of this method are the absence of sample preparation and rapid response (the measuring time is about 100 ms). The sensitivity of PTRMS is 100 ppt, and the storage time is 1 s. This approach is based on a gas-destructive method. Its major disadvantage is the narrow range of detectable substances. Specifically, it cannot be used for the analysis of such important EB components as small hydrocarbon molecules (alkanes, acetylene, ethylene) due to their low affinity for protons. Moreover, the total concentration of the substances that can be analyzed by PTRMS must not be higher than 10 ppm. The application of PTRMS, similarly to classical MS, encounters difficulties when it comes to the identification of the detected substances [65].

The further development of this approach constitutes a technique using a few reactants to ionize the substances to be detected (H_3O^+, NO^+, O_2^+) [66–69]. However, this method is less sensitive than PTRMS.

At present, the most promising option is a combination of MD and GC.

5.3 Gas chromatography/high-resolution mass spectrometry

GC/MS is most frequently used to analyze EB. Modern chromatographic columns allow up to 1,000 various compounds to be separated prior to their detection, which considerably enhances the accuracy and selectivity of the analysis. GC/MS separates substances to be determined from interfering 'highly intense' EB components, such as N_2, O_2, CO_2, and H_2O. The separated fractions are detected and analyzed by MS (Fig. 4).

Recent progress in GC/MS allowed combining it with time-of-flight detectors and double chromatographic separation. As a result, a measurement speed of 500 spectra per second was achieved instead of a few spectra per second attainable using a quadrupole mass spectrometer as the detector; this significantly decreased the time of analysis [70].

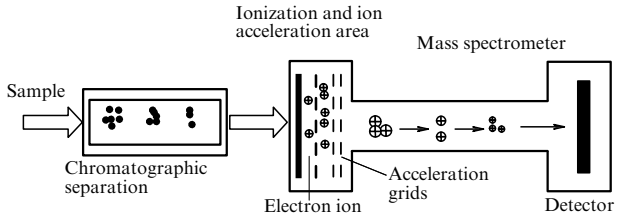

Figure 4. Block diagram of GC/MS.

GC/MS permits obtaining full high-resolution mass spectra for the time of peak formation, and the accurate measurement of ion masses allows determining the elemental composition of each ion in the mass spectrum [57]. Such an approach yields the maximum amount of structural information that can be deduced from the mass spectrum, i.e., a set of data on the exact elemental composition of ions and the relative intensity of their peaks. Moreover, MS helps to distinguish between substances with equal mass but different elemental compositions, which enhances the selectivity of detection.

Thus, the use of GC/MS for EB analysis allows determining the whole set of EB components with a sensitivity of the order of 1 ppb. Moreover, the possibility of selective detection ensures accurate measurement of individual EB components. These advantages of GC/MS promoted its wide application for EB analysis. A large class of marker gases, from carbon monoxide [71] to alkanes and other compounds, was discovered in EB using this method [72–74].

The disadvantages of GC/MS include the necessity of sample preparation and limitation of the analysis time to several minutes, needed for chromatographic separation of the gases, making GC/MS unsuitable for online measurements. As mentioned above, the use of a mass spectrometer as a detector encounters difficulties when it comes to the identification of substances with equal mass-to-charge ratios. Moreover, these apparatuses are cumbersome, expensive, and difficult to operate.

5.4 Infrared spectroscopy

Spectroscopy in the IR range has found especially wide application. This methods detects radiation passing through a sample, and the radiation intensity and spectrum contain information about the sample composition and concentration of individual components.

Under usual conditions, the relationship between the incident signal intensity J_0 and the intensity of radiation that passes through the absorbing medium, J, has the form

$$J = J_0 \exp(-\gamma l), \tag{1}$$

where l is the length of the absorbing medium and γ is the absorption coefficient of the sample. In the case of weak absorption ($\gamma l \ll 1$),

$$\gamma = \frac{J_0 - J}{J_0 l}, \tag{2}$$

and the absorption coefficient is related to the concentration of the substance as

$$\gamma = \sigma N, \tag{3}$$

where σ is the cross section of absorbing particles (cm^2) and N is the concentration (cm^{-3}).

Such an approach was most consistently realized in two apparatuses: the IR Fourier spectrometer and the diode laser-based spectrometer.

The IR Fourier spectrometer is most commonly used for gas analysis [75, 76]. A Fourier spectrometer (FS) refers to

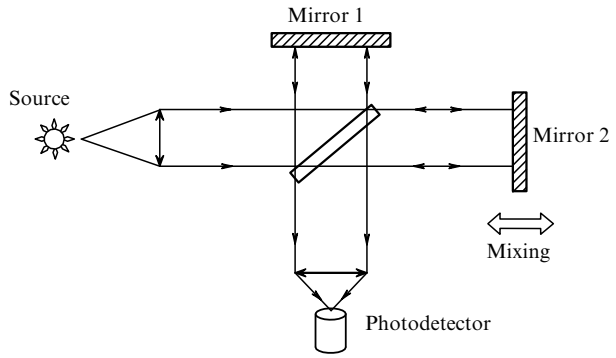

Figure 5. Schematic of a Michelson interferometer.

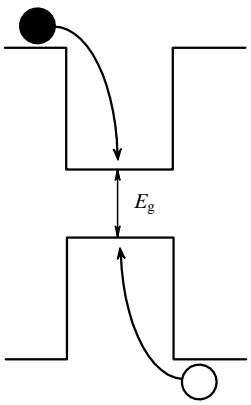

Figure 6. Principle of radiation generation in diode lasers.

modulation spectral instruments in which the spectrum is obtained by the inverse Fourier transform of an experimentally recorded signal. Such instruments are based on a device modulating the light flow in accordance with the radiation wavelength. As a rule, a classical two-beam Michelson interferometer is used, consisting of two mirrors, one of which is moveable, and a plate separating them (Fig. 5). As the mirror is moved, the photodetector records the spectral interferogram rather than the spectrum itself:

$$I(x) \sim \int_0^\infty B(v) \cos(2\pi v x)\, \mathrm{d}v\,, \tag{4}$$

where x is the displacement of the moveable mirror from the position corresponding to the zero optical path difference, v is the radiation frequency, and $B(v)$ is the sample spectrum. In fact, integration is performed over a finite wavenumber range due to the natural limitations on the spectral sensitivity of the photodetector and spectral transmission coefficient of the optical path. The initial spectrum is reconstructed by the inverse Fourier transform:

$$B(v) \sim \int_0^\infty I(x) \cos(2\pi v x)\, \mathrm{d}x\,. \tag{5}$$

Radiation sources in such apparatuses are either globars or mercury-vapor lamps, allowing extended spectra to be quickly obtained in order to register the absorption spectrum of many substances. However, the sensitivity of FS is low (below 0.1 pm), even using multipass cells, due to the low intensity of radiation sources.

The FS spectral sensitivity is constant over the entire working range of the spectrum and is determined only by the finite optical path difference L due to the moveable mirror,

$$\Delta v = \frac{q}{L}\,, \tag{6}$$

with the parameter $q = 0.5 - 2.0$. The size of diffraction gratings and prisms does not usually exceed 50 cm, which accounts for the limitation on spectral resolution at the level of 0.01 cm^{-1}.

Today, the market of gas analyzing equipment offers instruments whose operation is based on fundamental principles of diode laser absorption spectroscopy.

Tunable diode lasers (TDLs) are a class of semiconductor injection lasers in which the chemical composition of laser crystals, structure, and design features are intended to generate highly monochromatic ($\Delta v/v \approx 10^{-7}$) laser radiation tunable over a wide frequency spectrum [2, 77]. The TDL principle of action consists of direct conversion of the electric energy into optical radiation. Transmission of bias current through a semiconductor laser crystal in the forward direction leads to the injection of carriers (electrons and holes) into the p–n-transition zone, where a population inversion is thus created. Recombination of electrons (from the n-layer) and holes (from the p-layer) induces photon emission (Fig. 6).

Modern TDLs span a wide wavelength range from 0.6 to 40 μm containing absorption bands and lines of many known molecules. Such lasers have a power of 0.2–10 mW. One of their advantages is easy tuning in a wide generation frequency range by varying the temperature of the laser crystal, since the semiconductor bandgap determining the generation frequency depends on temperature. Because the forbidden bandgap and resonator eigenmode frequencies show different temperature dependences, TDL frequency tuning occurs in a piecewise continuous manner; in other words, continuous tuning regions alternate with 'silence' zones. The typical continuous tuning length of a single mode is 1–4 cm^{-1}. The length of the silence zone is roughly of the same order. The tuning range is such that it includes strong absorption bands of three or four gases at the most.

A decrease in the radiation linewidth and a single-mode generation regime can be reached by special methods (see, for instance, [77]), the most popular one being the introduction of distributed feedback (DFB). To this end, the profile of one of the heteroboundaries is made corrugated to ensure periodic variation of the refraction index and interference reflection of radiation (Fig. 7). The grating period is chosen so as to fulfil the Bragg condition for back reflection:

$$2n_e d = \lambda\,, \tag{7}$$

where λ is the wavelength, n_e is the effective refraction index of the active region, and d is the grating period.

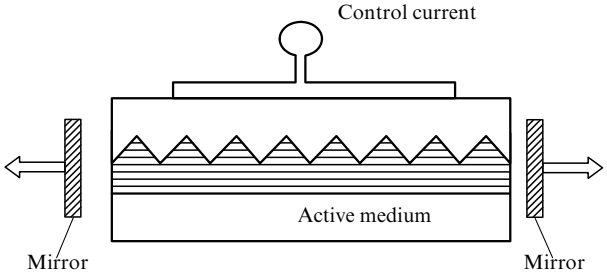

Figure 7. Schematic of a DFB laser.

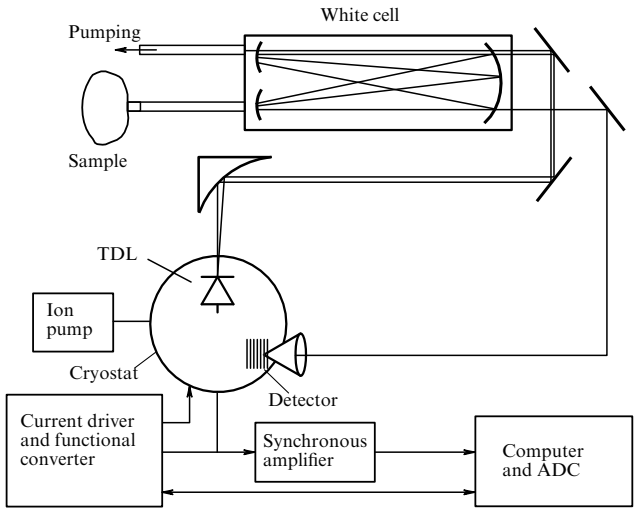

Figure 8. Block diagram of an IR spectrometer based on a tunable diode laser (TDL). ADC is a analog-to-digital converter.

The condition of reflection from a periodic structure is fulfilled for beams in both directions. In other words, the periodic grating creates a feedback in both directions, distributed along the entire TDL length. Such feedback being selective, a single-mode regime is maintained in DFB lasers. The typical width of the generation line is 1–10 MHz. Frequency tuning in DFB lasers is effected by varying the grating period.

The narrow generation line, high radiation power, and possibility of tuning determine the wide application of TDLs in spectroscopic research.

A typical TDL-based gas analyzer is shown in Fig. 8 [78]. A TDL is placed inside a closed-cycle cryostat. Laser radiation is fed into the White cell by a system of mirrors. The output signal is recorded by a photogalvanic detector located in the same cryostat. The laser is powered from a low-noise current driver. Frequency tuning is effected by saw-tooth voltage. The frequency is modulated by a triangular signal. Synchronous reception is realized with double frequency modulation. The signal is accumulated and processed in a computer block.

The sensitivity of such devices is limited by the inherent noise of the laser and photodetector. The TDL detection limit in the mid- and near-infrared regions determined by quantum noises of the laser and photodetector is described as the relative absorption level, $10^{-7}-10^{-8}$. Therefore, the practically attainable value is 10^{-6}, even with the use of the most sophisticated signal modulation and detection methods.

The use of high-Q resonators tuned to the frequency of a substance being detected increases the sensitivity of TDL spectroscopy to a few hundred ppt [79–82]. However, such analyzers have poor selectivity, because the resonator bandwidth may contain several absorption lines from different substances; therefore, their applications are limited to gas mixtures containing a small number of components.

Today, the application of TDL spectroscopy is limited to EB analysis for the presence of light molecules, such as CO, CO_2 [83–85], NO [86], ammonia [87, 88], acetone [89], methane [90], ethane [91, 92], and OCS [89, 93]; they are also used to determine the isotopic composition ($^{13}C/^{12}C$ ratio) [94].

To conclude this section, it is worth mentioning applications of quantum cascade lasers (QCLs) operating in the IR region. These are semiconductor lasers based on intersub-

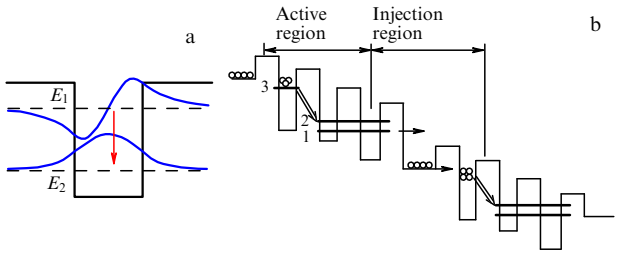

Figure 9. Principle of generating radiation in a quantum cascade laser.

band transitions in quantum wells [95]. Unlike interband optical transitions in diode lasers leading to electron–hole recombinations, all transitions in QCLs involve only electrons and occur between subbands of a single conduction band. In this case, the highest state density is concentrated in the transition energy E_{12}, since transitions in an active QCL medium occur between coupled electron states (Fig. 9a). The structure of the active QCL medium consists of alternating periods (usually, $N_p = 10-100$), each including two regions: an active region in which generation occurs and an injection (collector) region through which carriers propagate to reach the next active region. The active region includes at least three energy levels (Fig. 9b). Electrons from the neighboring region are injected into level 3. The population difference is maintained between levels 3 and 2, while transitions are accompanied by emission of a photon. The following condition must be satisfied for the population difference to exist:

$$\tau_{32} > \tau_2 , \qquad (8)$$

i.e., the total lifetime τ_2 of level 2 must be shorter than the time τ_{32} of transition from level 3 to level 2. Further, electrons pass from level 1 into the injection (collector) region. The main function of this region is to cool electrons and increase their energy in comparison with that of the edge of the energy band needed for successful injection in the next period.

The principle of cascade transitions provides two main advantages. First, the enlarged amplification region lowers the requirements for population density for each period and thereby decreases the threshold current. Second, each electron of the active medium can emit some N_p photons, which enhances the effectiveness of the device.

Modern QCLs operate in a wide IR region and generate a radiation power of a few tens of watts in the continuous generation regime [96–100]. The best characteristics are obtained for InGaAs/AlInAs/InP lasers in a wavelength range from 3.5 to 16 μm. QCLs are currently the only semiconductor lasers operating in the mid-IR range at room temperature. They are divided in terms of design into distributed feedback QCLs (DFB-QCLs) and external cavity QCLs (EC-QCLs).

DFB-QCLs are most frequently used in spectroscopic applications [101]. Their advantages include a small size, stable single-mode generation, and tunability without mode hopping. However, rapid frequency tuning by injection current is limited to the frequency range 2–3 cm^{-1}, while slow thermal tuning allows reaching the 10–20 cm^{-1} range. As far as EB analysis is concerned, this implies the possibility of recording absorption bands of at most two marker gases. The authors of [102] proposed broadening the tuning range by using an array of several QCLs and thereby increasing the frequency band overlap to 220 cm^{-1}. The main difficulty in

practical realization of this approach is that it requires spatial separation of the beams from different lasers.

Another way to address the problem of QCL narrow-band tuning is to use a grating-coupled external cavity to maintain the feedback between the laser and the frequency filter, i.e., to use an EC QCL.

The use of a grating for the single-mode generation regime at a wavelength of 5.1 μm and 84 K allowed obtaining the frequency band overlap of 54 cm^{-1} [103]; it could be extended to 91 cm^{-1} by means of additional thermal tuning. We note that this technique implies the use of additional devices and complicates operation of the laser.

Some authors described various IR QCL-based gas analyzers for EB analysis designed to detect well-known simple markers. For example, CO measurements by a pulsed DFB-QCL in the range 2176–2183 cm^{-1}, containing the strong vibrational band R(81) at 2176.2835 cm^{-1}, are reported in [104]. The same authors compared different spectrometer configurations to evaluate the possibility of achieving optimal sensitivity and selectivity. Figure 10a schematically depicts a spectrometer operating with long (100 ns) QCL pulses. A current pulse fed to the QCL produces a frequency chirp whose range is directly determined by the pulse length; it being ≈ 100 ns, the laser operates with a repetition rate of 10 kHz. QCL radiation traversing a multi-pass cell is recorded by an HgCdTe detector. The signal is transmitted from the detector to the preamplifier and then to the gated integrator, where it is discretized with a temporal integration window of 5 ns. Thereafter, the 3 Hz saw-tooth signal from the function generator scans each QCL pulse such that the full frequency scan is performed thrice every second.

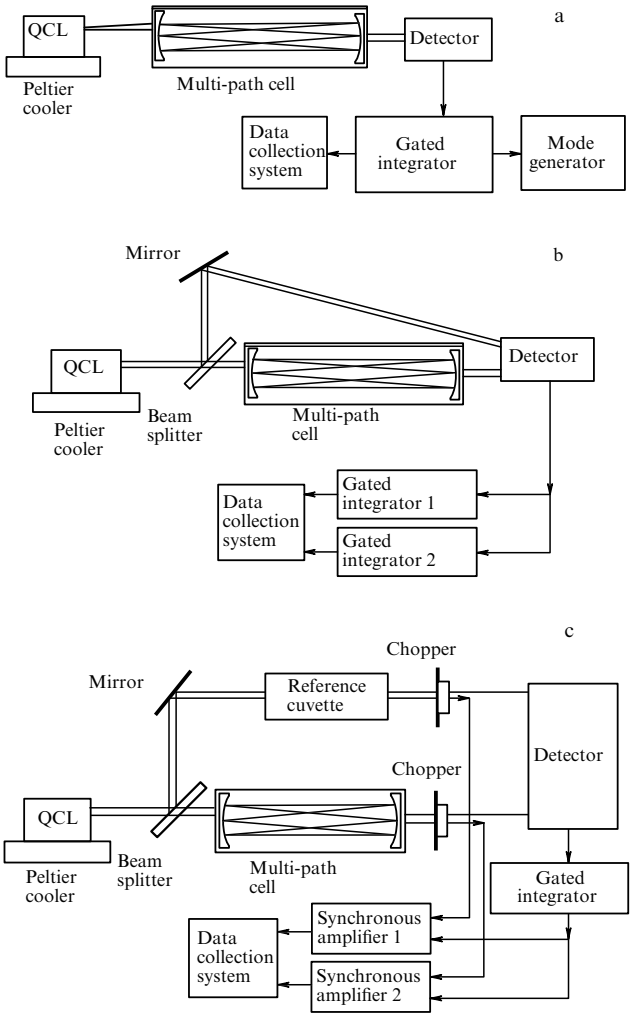

Figure 10. Various gas spectrometers with an IR QCL as the radiation source.

Measurements of the CO absorption line in a mixture with N_2 at 100 mbar indicate that the detection limit of such a device and the multi-path cell ensuring the beam path length 20 m is 1.2×10^{-5} cm^{-1}. The main factor limiting the sensitivity of the spectrometer is zero-line instability due to the irregular shape of the laser pulse: long pulse generation requires the maximum voltage, leading to the appearance of additional laser modes. Multi-mode radiation is in turn responsible for the irregular shape of the laser pulse registered by the detector and therefore for the zero-line instability.

To eliminate the multimode generation effect and decrease the QCL line width, a subthreshold voltage was used in the spectrometer shown in Fig. 10b; it resulted in a 20 ns pulse. Moreover, the beam was split into two by a ZnSe mirror to obtain a reference beam for recording and controlling the QCL pulse profile. The two beams were recorded by the detector and their intensity measured by the integrators. The use of short pulses allowed decreasing the contribution from the additional modes; thereby, the sensitivity of the method was improved to 8.2×10^{-7} cm^{-1} at the data accumulation time of 60 s, in accordance with the detection limit of 20 ppb. But the practically recorded minimal concentration of CO was 40 ppb. The discrepancy between theory and experiment was due to scan-to-scan fluctuations of the zero line and QCL frequency drift due to temperature. A disadvantage of such a gas analyzer is the limited rate of analysis due to the slow scanning frequency related to quiescent heat transfer.

The apparatus shown in Fig. 10c was designed to overcome this disadvantage. In this instrument, the QCL frequency is calibrated using a reference cell filled with pure CO, which permits the laser frequency drift with temperature to be taken into account. Then, compensation of the QCL frequency makes it possible to use signal registration in the time domain and avoid frequency scanning. In this case, the rate of analysis is determined by the detector inertness. An important component of such a scheme is the amplitude modulation of both beams (in this case, by two choppers). Modulation at two different frequencies allows the separation of the two signals in the frequency region and the elimination of the overlap effect.

The principles of modulation spectroscopy were used for the development of an NO sensor in Ref. [105]. The spectrometer described in [105] is based on DFB-QCL and has a wavelength of 5.2 μm (1891–1908 cm^{-1}) and a multi-pass cell ensuring an optical path of 76 m. This device is analogous to the TDL-based IR spectrometer in Fig. 8. The sensitivity of the sensor is a few ppb.

A photoacoustic spectrometer utilizing QCL for ammonia detection in EB is described in [106]. Its block diagram is presented in Fig. 11. The principle of its action consists of converting absorbed radiation into an electrical signal. Excitation of molecules by resonant radiation heats the gas and causes generation of a pressure pulse carrying information about the concentration of the molecules. Pressure differences change the microphone membrane capacitance and thereby generate the electrical signal [107]. The main

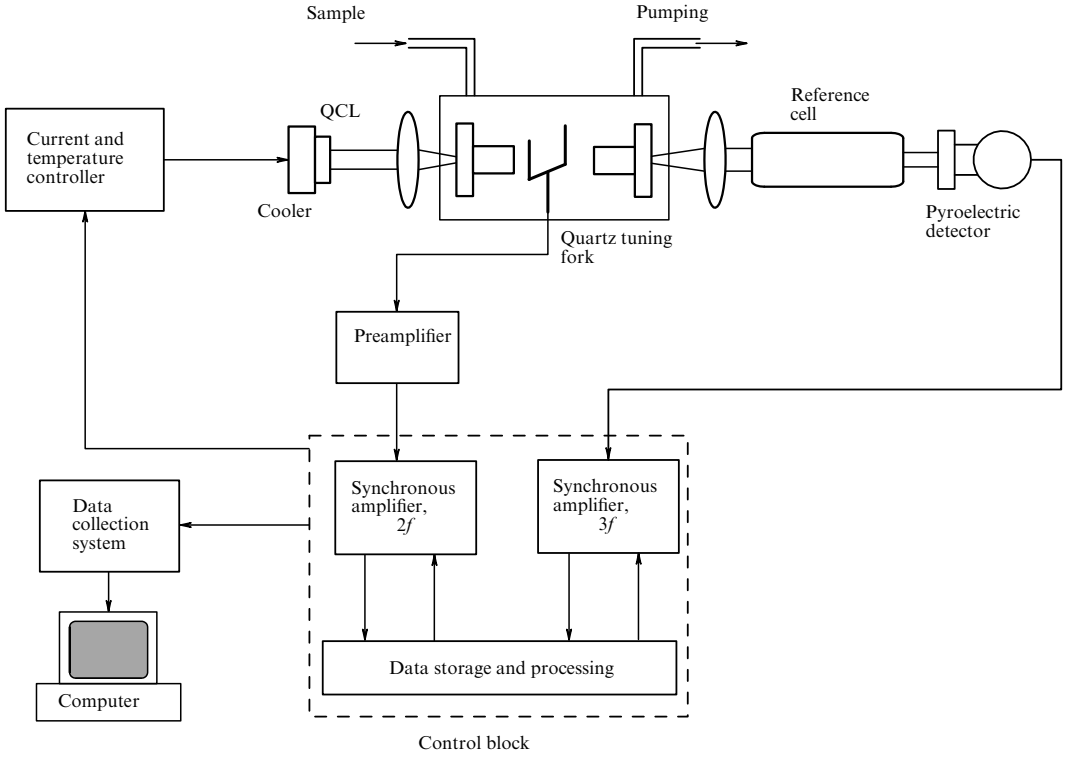

Figure 11. Block diagram of a photoacoustic spectrometer with a QCL.

advantage of photoacoustic spectrometers is a high sensitivity in terms of the absorption index ($10^{-9}-10^{-10}$ cm^{-1}). The limit sensitivity is determined by thermal fluctuations in the gas under study.

The optical sensor receiver (see Fig. 11) is a piezoelectric quartz tuning fork that allows eliminating the influence of environmental low-frequency acoustic noises. Moreover, the acoustic receiver provides a wide dynamic range of almost nine orders of magnitude. The signal-to-noise ratio can be increased roughly 30-fold using two $\lambda/2$ metallic microresonators, besides the quartz tuning fork. To increase the sensitivity of analysis, DFB-QCL radiation at 10.34 μm is stabilized in terms of frequency using the reference cell. The maximally detectable ammonia concentration is 6 ppb, with the accumulation time equaling 1 s.

Despite the fairly high sensitivity of such instruments, the use of DFB-QCLs permits detecting only one marker gas, which is a serious disadvantage of the method. As noted above, this can be overcome by using either an array of DFB lasers or an EC QCL. The development of methods for simultaneous detection of several marker gases is actually the main concern of groups working with IR QCLs. A few publications have reported the creation of such a technique. For example, the authors of [108] designed a sensor for the simultaneous detection of NO and CO_2 in EB based on two DFB-QCLs operating at 5.45 and 5.22 μm, respectively. Its sensitivity was enhanced by using a multi-path cell providing a path of several hundred meters. The sensitivity of NO detection is roughly 0.2 pb. The use of an EC QCL at a wavelength of 8.4 μm (with a tuning of 135 cm^{-1} and power of 50 mW) together with a photoacoustic spectrometer for the detection of acetone (1210 cm^{-1}) and freon-125 in a model mixture with nitrogen is described in [109]. This technique allowed the measurement of acetone and freon at the respective concentrations of 47.2 and 4.4 ppm.

5.5 High-resolution terahertz spectroscopy

The terahertz frequency range had until recently remained poorly known due to the lack of effective sources and receivers. The advent of various THz sources, including precious ones, gave a new impetus to the development of spectrometry and its applications [110–113]. At present, two approaches are available that permit fulfilling the requirements of EB analysis, to the utmost.

One is based on the use of a photomixer source [114–116]. The difference frequency of two continuous optical lasers is obtained with the help of a semiconductor mixer. A typical scheme of the photomixer spectrometer is presented in Fig. 12 [117]. The spectrometer has the following components: two optical (or infrared) lasers, a photomixer, a detector, and a cell with the gas to be analyzed.

Crucial for the development of such instruments is the choice of the lasers, which depends in the first place on the photomixer material determining the optimal laser wavelength. Usually, GaAs grown at a low temperature and showing strong absorption at ~ 820 nm is used. Other factors of importance for the choice of the lasers are the width of the generation line and the possibility of frequency tuning, which determine the spectral resolution and working range of the spectrometer. Successful operation of an optical laser is ensured when the linewidth is at least 1 MHz (for a single measurement time), attainable at a frequency stability level of 10^{-9}.

For example, Ti : Sa lasers feature a wide tuning range at a wavelength ≈ 800 nm and a linewidth of 100 kHz. However, their operation requires sophisticated control and tuning systems, as well as high-power pump lasers. An alternative to Ti : Sa lasers is compact EC-DLs with a wide tuning range. They also require control and frequency stabilizing systems, because the width of the generation line in EC-DLs is roughly 1 MHz per second due to jitter. The stabilizing system for one

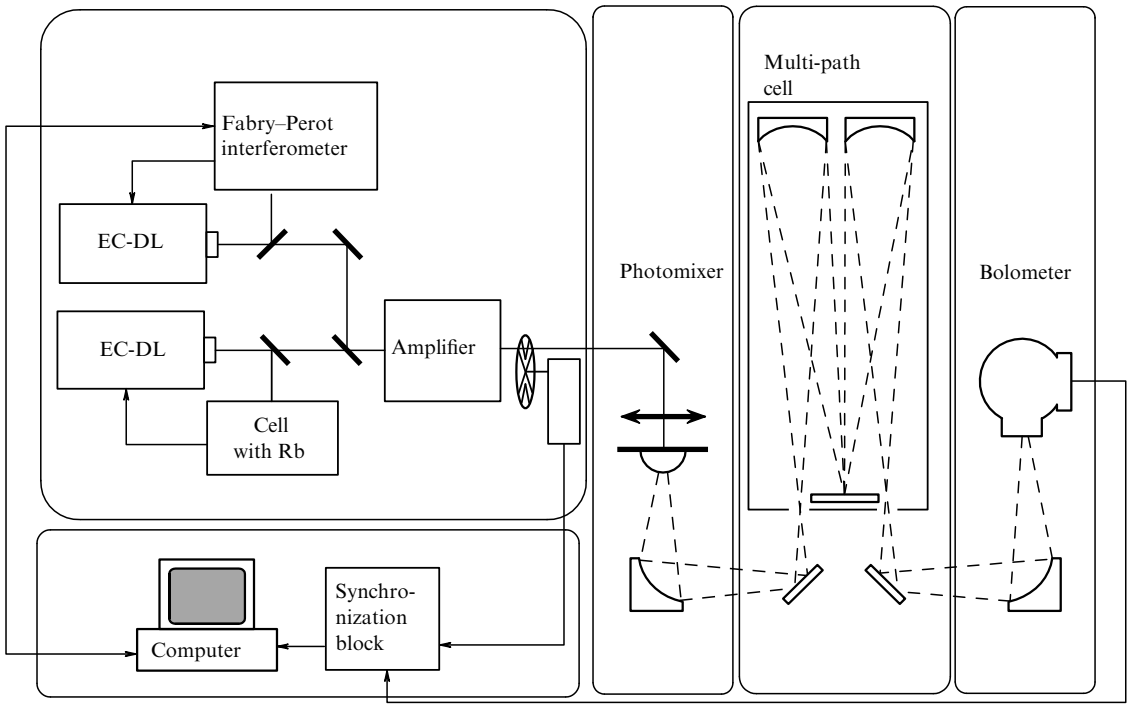

Figure12. Block diagram of a photomixer spectrometer.

of the two EC-DLs can be realized using Cs and Rb absorption lines at 842 and 780 nm transitions, which gives a linewidth of the order of 1 MHz. For the other laser, both frequency stability and tuning have to be ensured, with the possibility of their accurate measurement. One way to resolve this problem is to use a Fabry–Perot interferometer providing the desirable linewidth (~ 1 Hz) and allowing frequency scanning at 0.5 THz; however, only relative frequencies can be determined. Therefore, a frequency meter must be used to measure absolute frequencies with an error of 50 MHz, which makes it difficult to accurately determine the central frequencies of molecular transitions.

Another variant of self-tuning and scanning systems is the frequency comb generated by a sequence of short pulses from a stabilized laser. In this case, both DLs are locked to the nearest frequency comb mode (Fig. 13) [118], and THz radiation parameters depend on the repetition rate $f_{\rm rep}$ accuracy and stability. The use of the frequency comb permits obtaining a THz radiation wavelength of the order of 100 kHz. The simplest DL frequency scanning mechanism is gradual

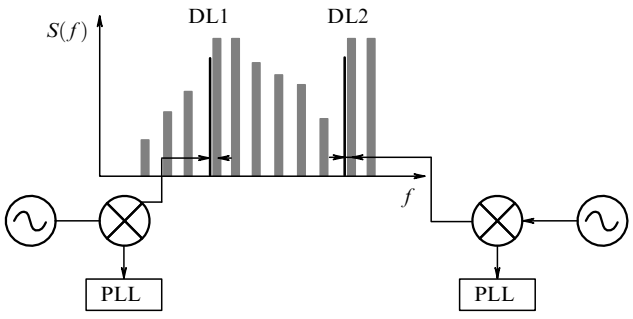

Figure 13. Principle of frequency stabilization of two diode lasers according to the frequency comb of a stabilized laser. PLL is a phase-lock loop system.

$f_{\rm rep}$ variation. However, it ensures frequency tuning of the order of 10 MHz; for this reason, frequency tuning with the help of a Fabry–Perot interferometer is used in applications.

As mentioned above, an advantage of this technique is the possibility of broad-band frequency tuning (0.5 THz) and spectral resolution of a few MHz. Such characteristics of the source permit recording absorption lines of several gases in a multi-component mixture, a crucial point for EB analysis. However, the radiation power of a photomixer is of the order of 1 μW (for frequencies above 1 THz) [117], which requires the use of highly sensitive receivers, largely cryogenic ones. Moreover, determination of absorption line central frequencies encounters difficulties. Today, such a technique is mostly used to detect simple substances, such as HCN, HCOOH (formic acid), CO, NO, and HCl [116, 117]; this permits reaching a sensitivity of several ppm, which is insufficient to detect many marker gases in EB.

One more line of development of precious THz spectrometers is related to traditional microwave physics. This approach utilizes a stable frequency generator created by multiplying the frequency of a highly stable reference synthesizer to ensure stable and accurate frequency setting at the 10^{-9} level of the carrier frequency. The key elements of such a system are frequency multipliers and mixers. Activities along this line date to the 1980s, when planar Schottky diodes were created [119].

The advent of new technologies in the past 10 years and the use of modern integrated circuit techniques resulted in a substantial improvement in the Schottky diodes for the entire subterahertz range [120]. Serial production of nonlinear elements based on planar Schottky diodes and radiation sources using them is currently underway. For example, Virginia Diodes (USA) manufactures 1.7 THz multipliers and 0.9 THz mixers, as well as radiation sources based on a solid-state frequency generator that operates in the 1.26–1.31 THz range with an output power of ≈ 10 μW [120, 121].

We note that the creation of multipliers based on Schottky diodes with a multiplication factor greater than 3 encounters difficulties at high frequencies. Evidently, the size of the Schottky diode must be small for work at high frequencies, which makes it difficult to design multipliers with the multiplication factor greater than 3. Higher multiplication factors are obtained using an array of multipliers with coefficients 2 and 3. Quantum semiconductor superlattices (SLs) have good prospects for application in photomultipliers with high harmonic numbers and other nonlinear elements [122]. A number of spectrometers with signal registration in the time domain were developed using microwave sources and frequency multipliers with SLs [123,124]. Spectrometers use the nonstationary effects of interaction between the gas and probing radiation. They register signals in the time domain.

Two operating modes can be realized in a spectrometer, phase switching and scanning the probe signal frequency. In the former mode, periodic radiation phase switch-over (with a π shift) resonantly interacting with the medium results in nonstationary emission and absorption, accounting for a periodic induction and decay of macroscopic polarization. Given a linear radiation–gas interaction, the processes of nonstationary radiation and absorption are readily distinguishable, because turning off the emission of radiation can be regarded as turning on radiation equal in modulus and opposite in phase. If the coherent spontaneous radiation (CSR) phase is opposite to the exciting radiation phase, the signal from temporal absorption can be regarded as CSR subtracted from the emission that passed through the absorption cell. Therefore, the phase switching signal can be represented as a superposition of two signals. One of them has an amplitude equal to the radiation source amplitude, and the other has twice that amplitude, and the opposite phase is amplitude-modulated by rectangular pulses. As soon as the second signal is switched on, the total signal undergoes phase reversal lasting as long as the amplitude remains constant. Clearly, the magnitude of the transmitted signal due to induction and delay of gas molecule polarization is twice that in field turning on/off processes used in spectrometers with frequency switching. Figure 14 illustrates the time dependence of the transmitted radiation power in the case of phase switching of microwave radiation with a power P_0 and a frequency ω_0.

Part of the diagram in Fig. 14 at $t < t_0$ corresponds to the stationary absorption mode ($P = P_0 - \Delta P$, where ΔP is the power absorbed by the molecules) and the induction of macroscopic polarization. Phase switching of radiation occurs at the instant $t = t_0$, and the quantum system falls out of resonance with the field. At this instant, $P = P_0 + \Delta P$. At $t < t_0$, the induced polarization decays, and the system returns to its initial state. The phase switching mode is typically used to detect a gas of interest in a mixture.

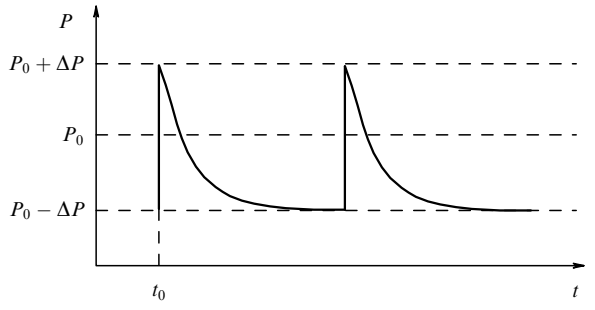

Figure 14. Signals of nonstationary emission and absorption from phase switching of radiation interacting with a gas.

To meet the requirements of high-resolution spectroscopy, the instantaneous values of the radiation source frequency for the phase switching mode must be set with an accuracy not worse than 10^{-8} with respect to the central radiation frequency. Such an accuracy can be attained by means of a phase-lock loop (PLL) system of the radiation source using a highly stable reference frequency synthesizer, providing spectral resolution at the level of 10 kHz, necessary for unambiguous registration and identification of the absorption lines of many gases.

A backward-wave oscillator (BWO) is used as the radiation source in the spectrometer (Fig. 15). The BWO is fed from a high-voltage source determining the generation frequency. A BWO signal passes through the cell containing an analyte gas and is registered by a Schottky diode detector. The detected signal is then amplified and transformed into a digital one in an analog-to-digital converter. Weak spectroscopic signals are distinguished from noise in real time as they are integrated and averaged at the input of a dedicated digital storage.

To realize the second operating mode, i.e., the fast frequency sweep of the probing signal, the following condition must be fulfilled in the linear approximation [125]:

$$\left|\frac{\mathrm{d}\omega}{\mathrm{d}t}\right| \gg \Gamma^2 , \tag{9}$$

where $\mathrm{d}\omega/\mathrm{d}t$ is the sweeping rate and Γ is the half-width of the molecular absorption line. We consider the sweeping described by a sawtooth curve (Fig. 16). The sweeping rate is then given by the expression

$$\mu = \frac{2(\omega_2 - \omega_1)}{T} . \tag{10}$$

The output signal is a superposition of the CSR signal at the molecular transition frequency ω_0 and the linear frequency-modulated (LFM) emission transmitted through the cell. The amplitude of the CSR signal is given by

$$E_{\mathrm{CSR}} \sim E_0 \gamma_0 l \Delta\omega_l \mu^{-1/2} g(t) , \tag{11}$$

where E_0 is the amplitude of probing radiation, γ_0 is the molecular absorption coefficient, l is the cell length, $\Delta\omega_l$ is the spectral line half-width, μ is the sweeping rate, and $g(t)$ is the pulse characteristic of the molecular absorption line. The spectroscopic signal, or temporal variations of the radiation amplitude at the cell outlet, is given by

$$\Delta E(t) \sim E_0 \gamma_0 l \Delta\omega_l \mu^{-1/2} g(t - t_0) \sin\frac{\mu(t - t_0)^2}{2} , \tag{12}$$

where t_0 is the time for which $\omega_l(t_0) = \omega_0$.

For $\gamma l \ll 1$, the output signal from the detector $U(t)$ is proportional to $\Delta E(t)$. The proportionality coefficient is determined by the detector parameters. Received spectroscopic signals $U(t)$ are reduced to a form characteristic of traditional pulsed Fourier spectrometers using the expression

$$U_1(t) = U(t)\cos\varphi(t) \pm H\big(U(t)\big)\sin\varphi(t) , \tag{13}$$

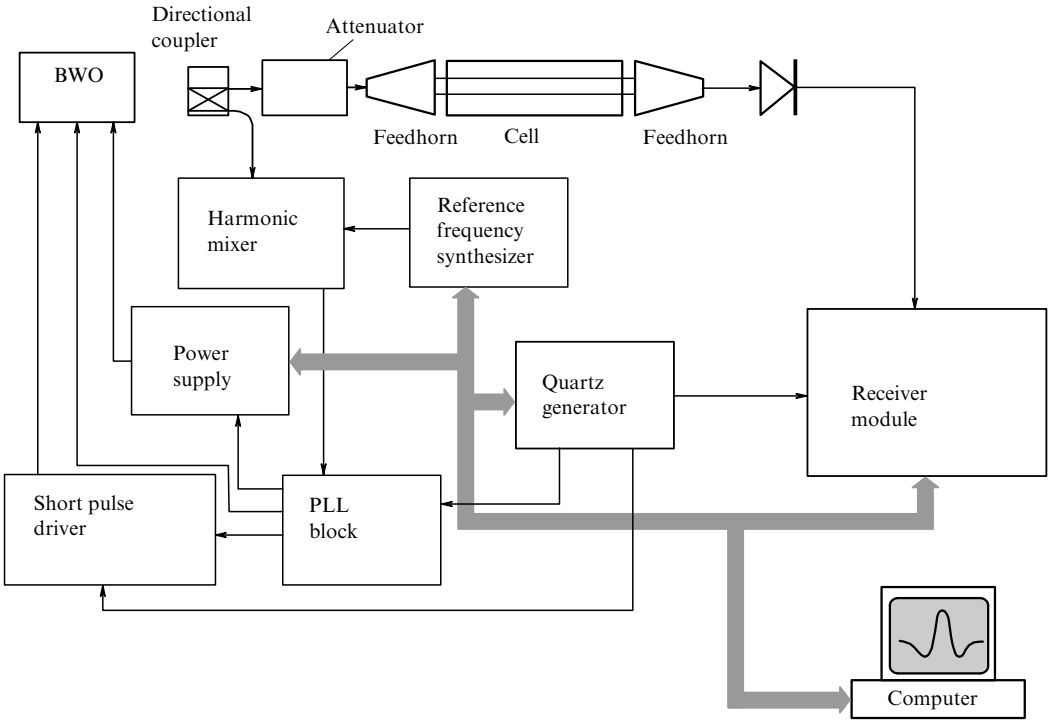

Figure 15. Block diagram of a THz spectrometer with phase switching of radiation interacting with a gas. BWO is a backward-wave oscillator.

where

$$\varphi(t) = \omega_1 t + \frac{\mu t^2}{2}, \quad 0 < t < \frac{T}{2},$$

$$\varphi(t) = \omega_2 t - \frac{\mu(t - T/2)^2}{2}, \quad \frac{T}{2} < t < T, \tag{14}$$

and $H(U(t))$ is the Hilbert transform:

$$H\big(U(t)\big) = -\frac{1}{\pi}\int_{-\infty}^{\infty} \frac{U(x)}{x - t}\,\mathrm{d}x. \tag{15}$$

Transformation (15) is used to obtain the $\pi/2$ phase shift for all components of the received signal. It can be realized as a combination of the following operations: Fourier transformation of the signal, interchange between the real and imaginary parts of the spectrum, and the inverse Fourier transformation.

Transformation (13) leads to

$$U_1(t) \sim E_0\gamma_0 l\Delta\omega_l \mu^{-1/2} g(t - t_0)\sin\left[(\omega_0 - \omega_1)(t - t_0)\right], \quad 0 < t < \frac{T}{2}, \quad t > t_0,$$

$$U_2(t) \sim E_0\gamma_0 l\Delta\omega_l \mu^{-1/2} g(t - t_0)\sin\left[(\omega_2 - \omega_0)(t - t_0)\right], \quad \frac{T}{2} < t < T, \quad t > t_0. \tag{16}$$

The Fourier transform of the signals obtained in both sweep half-periods and described by expression (16) yields an initial spectral characteristic of the absorption line with the central frequency $\omega_0 - \omega_1$ for $0 < t < T/2$ or $\omega_2 - \omega_0$ for $T/2 < t < T$. The resulting spectral line intensity is proportional to $\gamma_0 l\sqrt{\Delta\omega_l/\mu}$.

Characteristics obtained by signal transformation in the first and second sweep half-periods can be either analyzed separately or added to improve the signal-to-noise ratio. Such treatment yields a proper representation of the spectrum due to the linear character of operations and applicability of the superposition principle, even in the case of a large number of spectral lines within the scanning range.

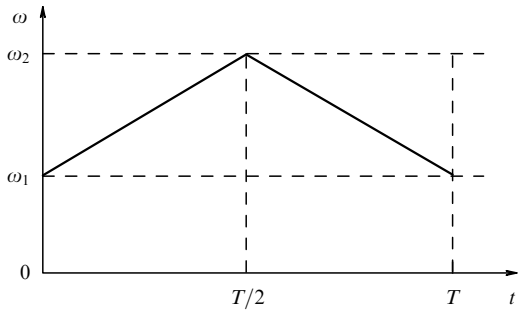

Figure 16. Frequency sweep characteristic.

Thus, the frequency scanning mode can be used to study the composition of a mixture or to simultaneously measure the concentrations of several gases. Wide-range measurements in the scanning mode allow simultaneously registering the absorption lines of several gases for a few fractions of a second. A block diagram of a fast frequency sweep spectrometer is presented in Fig. 17. The instantaneous values of the radiation source frequency must be set with an accuracy of at least 10^{-6}, as in the preceding case. This requirement is met with the help of a PLL system. The signal governing the BWO signal is fed either into the reference inlet of the high-voltage power supply unit or directly onto the BWO anode connected to the instrument case via a small resistor. Automatic tuning of the BWO frequency is performed against a highly stable reference frequency synthesizer. The sweep signal (voltage) governing the BWO frequency sweeping is generated by a high-speed 16-bit ADC. A signal similar to a triangular one is formed at the ADC outlet. The receiving part of the spectro-

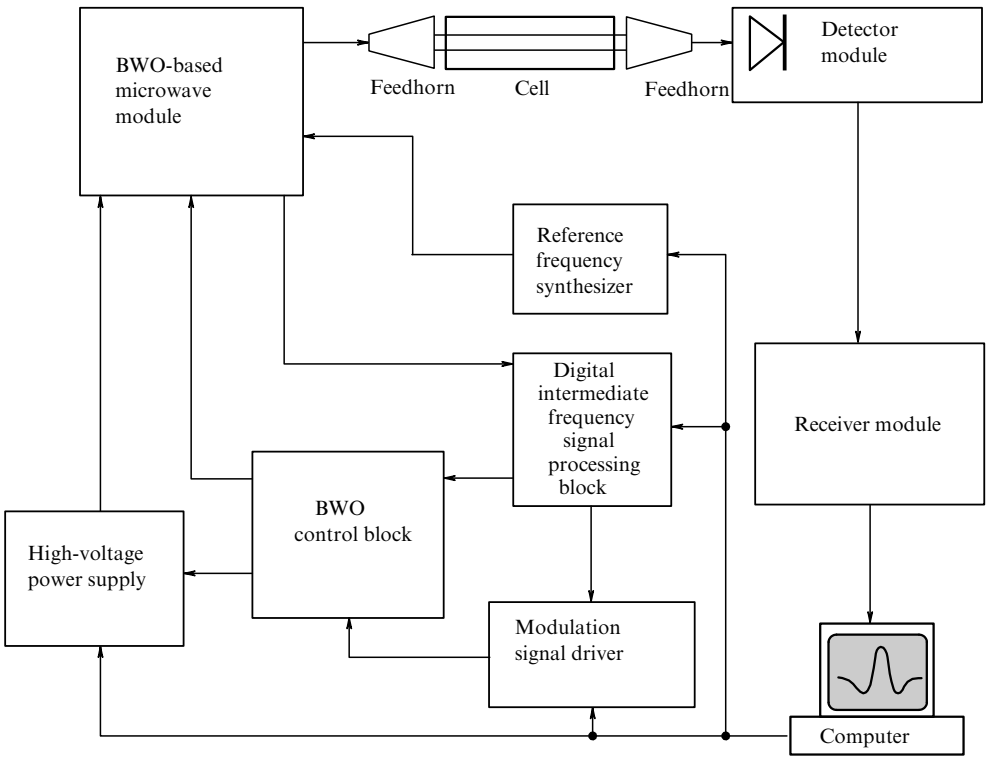

Figure 17. Block diagram of a fast frequency sweep spectrometer.

meter includes a detector module and a digital receiver module.

The detector module consists of a detecting head with a Schottky diode, a low-noise preamplifier with a bias feed circuit, and a low-pass filter (LPF). Measurement of the rectified constant voltage on the detector (at the LPF inlet) permits determining the spectral line intensity without preliminary calibration. The output signal from the preamplifier enters the high-speed ADC and, thereafter, the high-speed digital storage that integrates and averages spectroscopic signals in real time. Then the data are fed into a computer where averaging can be continued. Coherent accumulation of the signals allows increasing the signal-to-noise ratio and thereby enhancing the sensitivity of spectroscopic measurements.

Key components of the spectrometer are controlled by an inbuilt computer module that also processes spectroscopic signals.

Spectrometers using nonstationary effects are closest to the theoretical sensitivity limit with Doppler resolution. At the cell length $l = 1$ m and measurement time 1 s, the sensitivity of a spectrometer is 5×10^{-10} cm^{-1}. The accuracy of measuring the absorption line intensity (without preliminary calibration) is $\leqslant 5\%$. The accuracy of the frequency setting is 10^{-9} of the carrier frequency.

The application of THz spectrometers for the detection of the most important biomarkers in EB, such as nitric oxide, acetone, ammonia, and carbon monoxide, has been demonstrated in [126]. The sensitivity of THz spectrometers using nonstationary effects is still at the level of hundreds of ppb, but work on its improvement is underway.

To summarize, precious THz spectrometers ensure selective, reliable, and rapid measurements, as well as the possibility of simultaneously detecting a few marker gases. Further enhancement of their sensitivity in parallel with the development of compact and easy-to-operate instruments may provide a reliable method for EB analysis.

6. Conclusion

Extensive studies of the component composition of EB are currently underway at the intersection of medicine, physics, and chemistry. Despite numerous unresolved problems concerning the origin of many biomarkers, considerable progress in this field opens up new prospects for further research. Suffice it to say that strict requirements on the equipment for EB analysis stimulated the development of gas analysis technologies and resulted in the appearance of commercial analyzers for the detection of the simplest biomarkers. At the same time, a variety of high-priority technical problem that have to be addressed by physicists and engineers were identified for the wide application of diagnostic methods based on EB analysis in clinical settings. In this context, methods and instruments of THz spectroscopy appear to have especially good prospects, because they are free from many drawbacks inherent in other techniques described in this review.

The discovery of certain stable biomarkers of socially significant diseases gave an impetus to the development of a new technique known as metabolomic analysis. Its purpose is to study the multi-parameter response of the human body to genetic modifications, pathological stimulation, and environmental impacts. Such an approach implies identification of specific metabolites, e.g., the components of exhaled air, for the construction of a 'metabolic profile' of a concrete pathological condition.

The introduction of metabolomic analysis into clinical practice will allow recognizing subphenotypes of a concrete

disease and predicting the reaction of an organism to a given therapeutic modality. This will promote the formation of efficacious personalized medicine and contribute to the development of new methods for precision physical measurements and relevant equipment.

This study was supported by the Program of the Presidium of the Russian Academy of Sciences "Fundamental Sciences — Medicine," grant 11.G34.31.0066 of the government of the Russian Federation, and the TeraDec 047.018.005 project. It was also supported in part by the Skolkovo Institute of Science and Technology in the framework of the SkolTech/MIT Initiative.

References

1. Pauling L et al. *Proc. Natl. Acad. Sci. USA* **68** 2374 (1971)
2. Stepanov E V *Diodnaya Lazernaya Spektroskopiya i Analiz Molekul-Biomarkerov* (Diode Laser Spectroscopy and Analysis of Biomarker Molecules) (Moscow: Fizmatlit, 2009)
3. Pauwels R A, Rabe K F *Lancet* **364** 613 (2004)
4. Hurd S S, Pauwels R *Pulmonary Pharmacology Therapeutics* **15** 353 (2002)
5. National Asthma Education and Prevention Program, Expert Panel Report 2: Guidelines for the Diagnosis and Management of Asthma (NIH Publ., No. 97-4051) (Bethesda, MD: National Institute of Health, National Heart, Lung and Blood Institute, 1997); http://www.nhlbi.nih.gov/guidelines/archives/epr-2/asthgdln_archive.pdf
6. Fabbri L M, in *Breath Analysis Summit 2011, Intern. Conf. on Breath Research, 11–14 September 2011, Parma, Italy. Abstract Book* (Piacenza: Nuova Editrice Berti, 2011) p. 15
7. Alving K et al. *Eur. Respir. J.* **6** 1368 (1993)
8. Silkoff P E et al. *Chest* **119** 1322 (2001)
9. Dweik R A, in *Breath Analysis Summit 2011, Intern. Conf. on Breath Research, 11–14 September 2011, Parma, Italy. Abstract Book* (Piacenza: Nuova Editrice Berti, 2011) p. 27
10. "Recommendations for standardized procedures for the online and offline measurement of exhaled lower respiratory nitric oxide and nasal nitric oxide in adults and children — 1999" *Am. J. Respir. Crit. Care Med.* **160** 2104 (1999)
11. "ATS/ERS recommendations for standardized procedures for the online and offline measurement of exhaled lower respiratory nitric oxide and nasal nitric oxide, 2005" *Am. J. Respir. Crit. Care Med.* **171** 912 (2005)
12. George S C et al. *J. Appl. Physiol.* **96** 831 (2004)
13. Matthew M R et al. *J. Breath. Res.* **5** 016003 (2011)
14. Loukides S, in *Breath Analysis Summit 2011, Intern. Conf. on Breath Research, 11–14 September 2011, Parma, Italy. Abstract Book* (Piacenza: Nuova Editrice Berti, 2011) p. 59
15. Antczak A et al. *Respir. Med.* **94** 416 (2000)
16. Mazzone P *J. Breath Res.* **6** 027106 (2012)
17. "The National Lung Screening Trial: Overview and study design" *Radiology* **258** 243 (2010)
18. Hall W B et al. *Arch. Int. Med.* **169** 1961 (2009)
19. Iribarren C et al. *Am. J. Med.* **121** 989 (2008)
20. Phillips M et al. *Cancer biomarkers* **3** 95 (2007)
21. Gaspar E M et al. *J. Chromatogr. A* **1216** 2749 (2009)
22. Westhoff M et al. *Thorax* **64** 744 (2009)
23. Poli D et al. *Acta Biomed.* **79** (S1) 64 (2008)
24. Kischkel S et al. *Clin. Chim. Acta* **411** 1637 (2010)
25. Poli D, in *Breath Analysis Summit 2011, Intern. Conf. on Breath Research, 11–14 September 2011, Parma, Italy. Abstract Book* (Piacenza: Nuova Editrice Berti, 2011) p. 194
26. de Gennaro G et al. *Analyt. Bioanal. Chem.* **398** 3043 (2010)
27. Kazemi S et al. *J. Res. Med. Sci.* **16** 1097 (2011)
28. Wardi J et al. *J. Clin. Gastroenterology* **46** 293 (2012)
29. Redéen S et al. *Gastroenterology Res. Practice* **2011** 940650 (2011)
30. Vaks V L et al., in *Optika — XXI Vek. Mezhdunar. Kongress. Sb. Trudov Konf. "Fundamental'nye Problemy Optiki — 2010", Sb. Trudov Seminarov "Vserossiiskii Seminar po Teragertsovoi Optike i Spektroskopii", "Vserossiiskii Seminar po Opticheskim Metamaterialam, Fotonnym Kristallam i Nanostrukturam"* (Optics — XXI Century. The Intern. Congress. Proc. of the Conf. "Fundamental Problems of Optics — 2010", Proc. of the Seminar "All-Russian Seminar on Terahertz Optics and Spectroscopy", "All-Russian Seminar on Optical Metamaterials, Photonic Crystals and Nanostructures") Vol. 2 (Eds V G Bespalov, S A Kozlov) (St. Petersburg: ITMO, 2010) p. 382
31. Pelli M A (M.D.) et al. *Diseases Colon Rectum* **42** 71 (1999)
32. Dallinga J W et al., in *Breath Analysis Summit 2011, Intern. Conf. on Breath Research, 11–14 September 2011, Parma, Italy. Abstract Book* (Piacenza: Nuova Editrice Berti, 2011) p. 118
33. World Gastroenterology Organisation (WGO) Practice Guideline: Malabsorption, http://www.worldgastroenterology.org/assets/downloads/en/pdf/guidelines/13_malabsorption_en.pdf
34. Hamilton L H *Breath Test and Gastroenterology* 2nd ed. (Milwaukee, WI: QuinTron Instrument Co., 1998)
35. Altomare D F et al. *Brit. J. Surgery* **100** 144 (2013)
36. Galassetti P, in *Breath Analysis Summit 2011, Intern. Conf. on Breath Research, 11–14 September 2011, Parma, Italy. Abstract Book* (Piacenza: Nuova Editrice Berti, 2011) p. 111
37. Tisch U et al., in *Breath Analysis Summit 2011, Intern. Conf. on Breath Research, 11–14 September 2011, Parma, Italy. Abstract Book* (Piacenza: Nuova Editrice Berti, 2011) p. 157
38. Dorokhova E N, Prokhorova G V *Analiticheskaya Khimiya. Fiziko-Khimicheskie Metody Analiza* (Analytical Chemistry. Physicochemical Methods of Analysis) (Moscow: Vysshaya Shkola, 1991)
39. Bucca C et al. *J. Breath Res.* **6** 027104 (2012)
40. Perri F, Andriulli A (Eds) *Proc. Intern. Congress on Clinical Application of Breath Tests in Gastroenterology and Hepatology, Rome, 1998*, p. 212
41. Persson M G, Wilkund N P, Gustafsson L E *Am. Rev. Respir. Dis.* **148** 1210 (1993)
42. Bedfont Scientific Ltd: Gastrolyzer, http://www.bedfont.com/gastrolyzer
43. Ledochowski M et al. *Clin. Chim. Acta* **311** 119 (2001)
44. Low E C T, Ong M C C, Tan M *Singapore Med. J.* **45** 578 (2004)
45. Pisi R et al. *J. Asthma* **47** 805 (2010)
46. Chou J *Hazardous Gas Monitors: A Practical Guide to Selection, Operation and Applications* (New York: McGraw-Hill, 2000)
47. Gundermann K-D, McCapra F *Chemiluminescence in Organic Chemistry* (Berlin: Springer-Verlag, 1987)
48. García-Campaña A M, Baeyens W R G (Eds) *Chemiluminescence in Analytical Chemistry* (New York: Marcel Dekker, 2001)
49. Oh K S, Woo S I *Sci. Technol. Adv. Mater.* **12** 054211 (2011)
50. Artlich A et al. *Biol. Neonate* **79** 21 (2001)
51. Silkoff Ph *J. Breath Res.* **2** 037001 (2008)
52. Cristescu S M et al. *J. Breath Res.* **7** 017104 (2013)
53. Silkoff P E et al. *J. Allergy Clin. Immunol.* **114** (5) 1241 (2004)
54. Boot J D et al. *Respiratory Med.* **102** 1667 (2008)
55. de Lacy Costello B P J, Ewen R J, Ratcliffe N M *J. Breath Res.* **2** 037011 (2008)
56. Stetter J R, Penrose W R, Yao Sh *J. Electrochem. Soc.* **150** S11 (2003)
57. Khmel'nitskii R A, Brodskii E S *Khromato-Mass-Spektrometriya* (Chromatomass-Spectrometry) (Ser. "Methods of Analytical Chemistry") (Moscow: Khimiya, 1984)
58. Esterbauer H *Pathol. Biol.* **44** 25 (1996)
59. Zemskov V S, Khrapach V V, Liashenko V A *Klin-Khir.* **11** 9 (1992)
60. Tangerman A et al. *J. Breath Res.* **6** 017102 (2012)
61. Beyermann K *Organic Trace Analysis* (Stuttgart: Georg Thieme Verlag, 1982); Translated into Russian: *Opredelenie Sledovykh Kolichestv Organicheskikh Veshchestv* (Moscow: Mir, 1987)
62. Schwarz K et al. *J. Breath Res.* **3** 027003 (2009)
63. Taucher J et al. *Rapid Commun. Mass Spectrom.* **11** 1230 (1997)
64. Blake R S *Analyt. Chem.* **76** 3841 (2004)
65. Herbig J et al. *J. Breath Res.* **3** 027004 (2009)
66. Spanel P, Smith D *Eur. J. Mass Spectrom.* **13** 77 (2007)
67. Boshier P R et al. *Analyst* **136** 3233 (2011)
68. Smith D, Spanel P *Trends Analyt. Chem.* **30** 945 (2011)
69. Dummer J F et al. *J. Breath Res.* **4** 046001 (2010)
70. Amann A et al. *Eur. Respir. Soc. Monograph* **49** 96 (2010)
71. Matthews D E, Hayes J M *Analyt. Chem.* **50** 1465 (1978)
72. Phillips M et al. *Lancet* **353** 1930 (1999)
73. Phillips M et al. *J. Breath Res.* **4** 026003 (2010)

74. Fuchs P et al. *Int. J. Cancer* **126** 2663 (2010)
75. Griffiths P R, de Haseth J A *Fourier Transform Infrared Spectrometry* 2nd ed. (Hoboken, NJ: Wiley-Intersci., 2007)
76. Morozov A N, Svetlichnyi S I *Osnovy Fur'e-Spektroradiometrii* (Fundamentals of Fourier Spectroradiometry) (Moscow: Nauka, 2006)
77. Nasim H, Jamil Ya *Laser Phys. Lett.* **10** 043001 (2013)
78. Roller Ch et al. *Appl. Opt.* **41** 6018 (2002)
79. Schmidt F M et al. *J. Breath Res.* **5** 046004 (2011)
80. Paldus B, Kachanov A, in *Handbook of Atomic, Molecular, and Optical Physics* (Ed. G Drake) (Berlin: Springer-Verlag, 2006) p. 633
81. Fritsch Th, Hering P, Mürtz M *J. Breath Res.* **1** 014002 (2007)
82. Heinrich K et al. *Appl. Phys. B* **95** 281 (2009)
83. Wang C *Sensors* **9** 8230 (2009)
84. Crosson E R et al. *Analyt. Chem.* **74** 2003 (2002)
85. Ivashkin V T et al. *Tr. Inst. Obshch. Fiz. im. A M Prokhorova* **61** 253 (2005)
86. Roller Ch et al. *Appl. Opt.* **41** 6018 (2002)
87. Lachish U et al. *Rev. Sci. Instrum.* **58** 923 (1987)
88. Kosterev A A, Tittel F K *Appl. Opt.* **43** 6213 (2004)
89. Wojtas J et al. *Opto-Electron. Rev.* **20** 26 (2012)
90. D'Amato F, Mazzinghi P, Castagnoli F *Appl. Phys. B* **75** 195 (2002)
91. Skeldon K D *Respir. Med.* **100** 300 (2006)
92. Skeldon K et al. *Appl. Opt.* **44** 4712 (2005)
93. Halmer D et al. *Opt. Lett.* **30** 2314 (2005)
94. Becker J F *Appl. Opt.* **31** 1921 (1992)
95. Faist J et al., in *Mid-Infrared Coherent Sources and Applications* (Eds M Ebrahim-Zadeh, I T Sorokina) (New York: Springer, 2008) p. 171
96. Scalari G et al. *Laser Photon. Rev.* **3** 45 (2009)
97. Zeller W et al. *Sensors* **10** 2492 (2010)
98. Bai Y et al. *Appl. Phys. Lett.* **99** 261104 (2011)
99. Lu Q Y et al. *Appl. Phys. Lett.* **98** 181106 (2011)
100. Bai Y et al. *Appl. Phys. Lett.* **98** 181102 (2011)
101. Guimbaud C *Measur. Sci. Technol.* **22** 075601 (2011)
102. Lee B G *IEEE Photon. Technol. Lett.* **21** 914 (2009)
103. Luo G P *IEEE J. Quantum Electron.* **38** 486 (2002)
104. Moeskops B *Appl. Phys. B* **82** 649 (2006)
105. J Mandon et al. *J. Biomed. Opt.* **17** 017003 (2012)
106. Lewicki R et al. *Proc. SPIE* **7945** 79450K (2011)
107. Kozintsev V I et al. *Lazernyi Optiko-Akusticheskii Analiz Mnogokomponentnykh Gazovykh Smesei* (Laser-Assisted Optico-Acoustic Analysis of Many-Component Gas Mixtures) (Moscow: MGTU im. N E Baumana, 2003)
108. McCurdy M R *J. Biomed. Opt.* **12** 034034 (2007)
109. Lewicki R et al. *Opt. Express* **15** 7357 (2007)
110. Dexheimer S L (Ed.) *Terahertz Spectroscopy: Principles and Applications* (Boca Raton: CRC Press, 2008)
111. Bründermann E, Hübers H-W, Kimmitt M *Terahertz Techniques* (Heidelberg: Springer, 2012)
112. Bratman V L, Litvak A G, Suvorov E V *Phys. Usp.* **54** 837 (2011); *Usp. Fiz. Nauk* **181** 867 (2011)
113. Mukhin A A et al. *Phys. Usp.* **52** 851 (2009); *Usp. Fiz. Nauk* **179** 904 (2009)
114. Brown E R *Proc. SPIE* **7938** 793802 (2011)
115. Preu S et al. *J. Appl. Phys.* **109** 061301 (2011)
116. Park I et al. *Meas. Sci. Technol.* **19** 065305 (2008)
117. Hindle F et al. *Sensors* **9** 9039 (2009)
118. Mouret G et al. *Opt. Express* **17** 22031 (2009)
119. Bishop W L et al., in *Proc. IEEE MTT-S Intern. Microwave Symp., Las Vegas, USA, June 9–11, 1987*, p. 607
120. Weikle R M, Crowe T W, Kollberg E L *Int. J. High Speed Electron. Syst.* **13** 429 (2003)
121. Virginia Diodes, Inc., http://vadiodes.com/
122. Winnerl S et al. *Phys. Rev. B* **56** 10303 (1997)
123. Vaks V *J. Infrared Millimeter Terahertz Waves* **33** 43 (2012)
124. Vaks V L et al. *Radiophys. Quantum Electron.* **51** 493 (2008); *Izv. Vyssh. Uchebn. Zaved. Radiofiz.* **51** 490 (2008)
125. Khodos V V, Ryndyk D A, Vaks V L *Eur. Phys. J. Appl. Phys.* **25** 203 (2004)
126. Vaks V L et al. *J. Opt. Technol.* **79** 66 (2012); *Opt. Zh.* **79** (2) 9 (2012)
127. Vaks V et al. *J. Appl. Phys.* **111** 074903 (2012)
128. Vaks V L et al. *Phys. Solid State* **52** 2241 (2010); *Fiz. Tverd. Tela* **52** 2100 (2010)